### Title
Finite Element Analysis of Mechanical Ocular Sequelae from Badminton Shuttlecock Projectile Impact.




### Journal
Ophthalmology Science, 5(1)



### Authors
Hong, John
Colmenarez, Jose
Choi, Elliot
et al.



### Publication Date
2025

### DOI
10.1016/j.xops.2024.100625

Peer reviewed

AMERICAN ACADEMY OF OPHTHALMOLOGY®

# Finite Element Analysis of Mechanical Ocular Sequelae from Badminton Shuttlecock Projectile Impact

John D. Hong, PhD,[1,*] Jose A. Colmenarez, MS,[2,*] Elliot H. Choi, MD, PhD,[1] Alex Suh, BS,[3] Andrew Suh, BS,[3] Matthew Lam, MD,[4] Annette Hoskin, PhD,[5,6] Don S. Minckler, MD, MS,[1] Ken Y. Lin, MD, PhD,[1] Kourosh Shahraki, MD,[1] Rupesh Agrawal, MD,[7,8,9,10] Pengfei Dong, PhD,[2] Linxia Gu, PhD,[2] Donny W. Suh, MD, MBA[1]

***Purpose:*** With the growing popularity of badminton worldwide, the incidence of badminton-related ocular injuries is expected to rise. The high velocity of shuttlecocks renders ocular traumas particularly devastating, especially with the possibility of permanent vision loss. This study investigated the mechanism behind ocular complications through simulation analyses of mechanical stresses and pressures upon shuttlecock impact.

***Design:*** Computational simulation study.

***Participants:*** None.

***Methods:*** A 3-dimensional human eye model was reconstructed based on the physiological and biomechanical properties of various ocular tissues. Finite element analysis simulations involved a frontal collision with a shuttlecock projectile at 128.7 km/hour (80 mph). Intraocular pressure (IOP) changes and tissue stress were mapped and quantified in the following ocular structures: the limbus, ciliary body, zonular fibers, ora serrata, retina, and optic nerve head.

***Main Outcome Measures:*** Intraocular pressure and tissue stress.

***Results:*** Upon shuttlecock impact, compressive force was transferred to the anterior pole of the cornea, propagating posteriorly to the optic nerve head. Deflection of forces anteriorly contributed to refractory oscillations of compressive and tensile stress of ocular tissue. Initial impact led to a momentary (<1 ms) spike in IOP 5.66 MPa ($42.5 \times 10^3$ mmHg) that radially distributed for a very brief instance (<1 ms) of pressure at the trabecular meshwork of the iridocorneal angle of 1.25 MPa ($9.4 \times 10^3$ mmHg). The lens had a maximal posterior displacement of 1.5 mm with peak zonular fiber tensile strain of 52%. The limbus, ciliary body, and ora serrata had a peak tensile stress of 5.16 MPa, 1.90 MPa, and 0.62 MPa, respectively. Compressive force from the sclera concentrated at the optic nerve head for a peak stress of 5.97 MPa while peak pressure from vitreous humor was 7.99 MPa.

***Conclusions:*** Shuttlecock impact led to a very brief, substantial rise in pressure and stress significant for tissue damage and subsequent complications, such as secondary glaucoma, angle recession, lens subluxation, hyphema, or retinal dialysis. Our findings offer valuable mechanistic insights into how ocular structures are affected by shuttlecock projectile impact to inform clinical assessments and treatment strategies, while highlighting the importance of protective eyewear in racket sports.

***Financial Disclosures:*** Proprietary or commercial disclosure may be found in the Footnotes and Disclosures at the end of this article. *Ophthalmology Science 2025;5:100625* 

*Supplemental material available at www.ophthalmologyscience.org.*

Badminton is among the most popular racquet sports played with a projected 339 million active players worldwide.[1] With an increasing number of players each year, the incidence of badminton-related injuries is expected to rise, with injuries to the eye being among the most devastating. Shuttlecocks are the primary cause of badminton ocular injuries, with the majority of patients presenting with complaints of visual impairment during their initial hospital visit.[2–6] Approximately half of badminton-related eye injuries have resulted in permanent vision loss, with up to a quarter with a reported final visual acuity of <6/60.[3,5,7]

Blunt ocular trauma caused by shuttlecock impact poses significant risks due to its high velocity and abrupt changes in direction and speed. Higher levels of competition are



https://doi.org/10.1016/j.xops.2024.100625
ISSN 2666-9145/24

associated with greater risk due to faster shuttlecock velocities.[8] Shuttlecock speeds typically average 168 to 217 km/h, transferring about 6 to 9 J of force to the eye.[9,10] Peak initial velocity has been recorded at 493 km/hour.[11] Furthermore, the head of the shuttlecock (25 mm in diameter) is similar in size to the eye (24 mm in diameter); therefore, the projectile force would be transferred directly to the eye without the support of the orbit to cushion the impact.[12] Additionally, the lack of protective eyewear among recreational and professional players further increases the risk of ocular injury during badminton play.[8,13]

The region most prone to injury from badminton was found to be zone II of the eye, specifically the limbus and deeper structures, such as the ciliary body and muscles, trabecular meshwork, zonular fibers, and ora serrata.[14] Though closed globe injuries account for almost all shuttlecock eye injuries, a few open globe injuries have also been reported.[2,3,14] Ocular complications from badminton-related injuries include: hyphema, traumatic mydriasis, traumatic angle recession, anterior uveitis, secondary glaucoma, optic nerve avulsion, lens subluxation, traumatic cataracts, cyclodialysis, iridodialysis, vitreous hemorrhage, commotio retinae, retinal dialysis or detachment, and retinal hole.[3,4,10,14–18] These injuries can have serious and long-term consequences for the affected individual, including vision impairment and blindness.

To understand how shuttlecock impact can cause these ocular complications, investigating the mechanistic intricacies underlying the distribution of forces upon impact to the anterior and posterior segment of the eye becomes crucial. This understanding can shed light on why specific ocular structures are more vulnerable to damage, thereby guiding clinical assessments and treatment strategies after blunt ocular trauma. By delineating the precise biomechanical pathways involved, clinicians can better anticipate potential damage to ocular structures and tailor their assessments to evaluate the integrity and function of these structures more effectively. Additionally, such insights can aid in the development of targeted preventive measures aimed at mitigating the risk of ocular injury during badminton play, including the promotion of protective eyewear and the implementation of training programs to enhance player awareness and safety protocols. Ultimately, this interdisciplinary approach bridges biomechanics with clinical practice, fostering advancements in ocular health and injury prevention within the realm of sports medicine.

Given the challenges of quantitatively investigating in vivo shuttlecock-induced ocular injuries in human subjects, our study explores the dispersion of mechanical forces through the eye imparted by shuttlecock impact using finite element analysis (FEA) simulations. Finite element analysis simulations use a human eye model composed of block-like elements assigned with appropriate physiologic mechanical properties.[19] Finite element analysis has been used for mechanistic studies of other ocular traumatic injuries, such as abusive head trauma, soccer ball impact, basketball impact, intrapartum fetal head compression, and blast wave from explosives.[19–25] In our study, projectile impact from a shuttlecock is applied to simulate the consequent outcome in the model eye. The simulation quantifies and maps the spatial and temporal distribution of biomechanical stress throughout the eye, as well as fluctuations in intraocular pressure (IOP), upon shuttlecock impact. Our study highlights ocular structures particularly at risk of significant damage after badminton-related injury.

## Methods

### Computational Simulation of Badminton Shuttlecock Impact

Finite element analysis was conducted on an eye model to simulate the biomechanical response to the impact of a badminton shuttlecock. A 3-dimensional model human eye was constructed based on our previous studies investigating soccer ball trauma, intrapartum fetal head compression, and abusive head trauma.[19,21,24] The model human eye in our study was composed of the cornea, sclera, choroid, lens, ciliary body, zonular fibers, aqueous humor, vitreous, retina, and optic nerve (Fig 1). The model also included surrounding orbital fat and bone. The badminton shuttlecock was modeled as a rigid silo-shaped tip with a diameter of 25 mm. The shuttlecock velocity was set at 80 mph (129 km/hour) to emulate conditions between the reported average and terminal velocities.[9,26] A frontal collision to the cornea at a direct zero-degree impact angle was considered for the simulation.

The physiologic biomechanical properties of each ocular tissue were obtained from literature.[19,27–35] A summary of the tissue properties can be found in supplementary table 1 (available at www.ophthalmologyscience.org). To simulate the fluid-structure interaction between the aqueous and vitreous humors, we implemented coupled Eulerian–Lagrange elements. The orbit was fixated at the base of the intracanalicular region to mimic its stable positioning within the head, attributable to its integration with the rigid skull and supportive tissues. An initial pressure of 2.8 kPa (21 mmHg) was exerted toward the inner surface of the aqueous and vitreous cavities to model the physiological IOP values of a healthy eye. Contact interactions between the shuttlecock and the eye were established utilizing a frictionless penalty method. The simulation was performed in the FEA solver ABAQUS/Explicit 2023 (Dassault Systemes Simulia Corp), with a designated impact time of 3 ms, enough to capture the contact and rebounding of the shuttlecock in the eye. In total, 544 210 elements were employed to mesh both the eye and shuttlecock. Stress and stretch measurements were collected for the structures composing the posterior and anterior poles of the globe for their analysis.

## Results

The simulation of shuttlecock impact demonstrated transmission of compressive force from the anterior pole at the cornea to the posterior pole at the optic nerve head (Fig 2). The force is deflected anteriorly, causing multiple interfering translational pressure waves through the eye. The stress heatmap shows immediate transmission of force from the shuttlecock to the anterior chamber within a fraction of a millisecond, followed by immediate dispersion of forces down to the optic nerve head (Fig 2). The complete simulated biomechanical deformation of the model eye as well as corresponding stress heatmap simulations are demonstrated in supplementary media S1 to S2 (available at www.ophthalmologyscience.org).

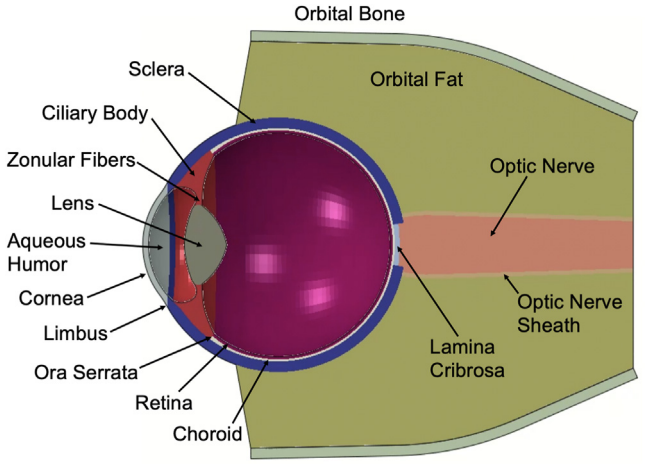


**Figure 1.** Finite element analysis human eye model cross-sectional view. The model eye was constructed with elements based on parameters from prior FEA model eyes.[19,21] FEA = finite element analysis.

Notably, the shuttlecock continues to push on the cornea and compress the anterior chamber until making impact with the limbus and ciliary body, which provide the stopping force preventing the shuttlecock from advancing further. Upon neutralizing the force of impact through the opposing force exerted by the eye structure, equilibrium is achieved. Consequently, the shuttlecock rebounds due to the inherent elasticity of the globe. During this process, the limbus sustains an initial compressive stress of 2.08 MPa upon the cornea buckling (Fig 3). When the impact wave front passes through the limbus and the cornea reaches its maximal deformation point, the limbus experiences an elevated tensile stress of 5.03 MPa (Fig 3). Then, the stress decreases, showing a compressive response, as the shuttlecock decelerates and separates from the eye. Finally, the stress reaches another tensile peak of 0.5 MPa as the cornea is returning to its original shape due to its elasticity, from which it decays to 0. The corresponding simulations are demonstrated in supplementary media S3 (available at www.ophthalmologyscience.org).

Shuttlecock impact and resultant compressive force to the anterior chamber causes posterior lens displacement, with a maximal movement of 0.5 mm at the 0.2-ms juncture (Fig 4). Correspondingly, there is a maximal tensile stress to

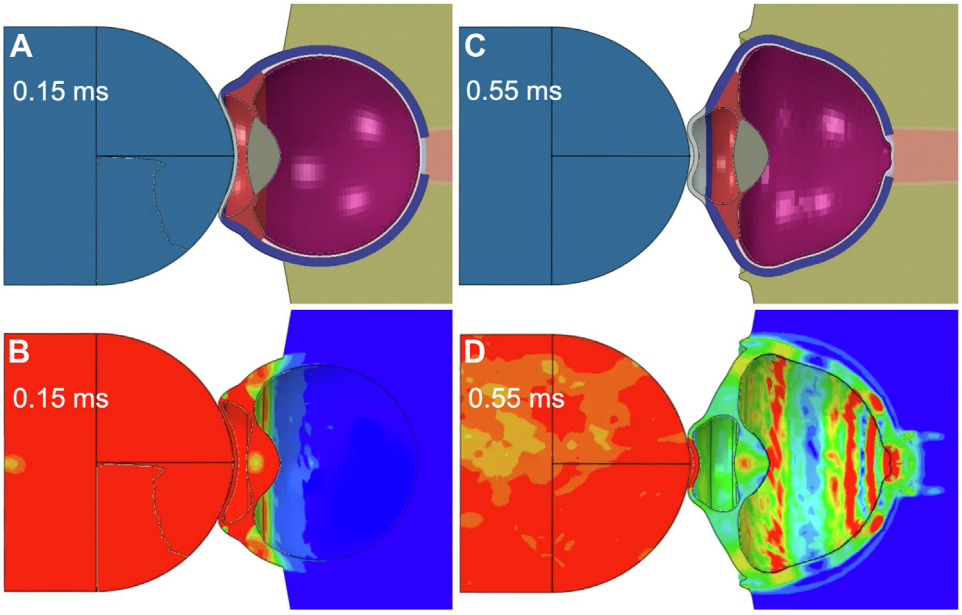


**Figure 2.** Distribution of shuttlecock mechanical force through the eye over time. **A,** Initial stages of transfer of mechanical force from shuttlecock impact. **B,** Stress heatmap of the anterior chamber structures and sclera during initial stages. **C,** Subsequent propagation of mechanical force through the eye with axial contraction. **D,** Corresponding stress heatmap of anterior chamber and sclera with propagation of pressure down to the optic nerve head. The simulation of shuttlecock impact and corresponding stress heatmaps are shown by Supplementary Media 1.

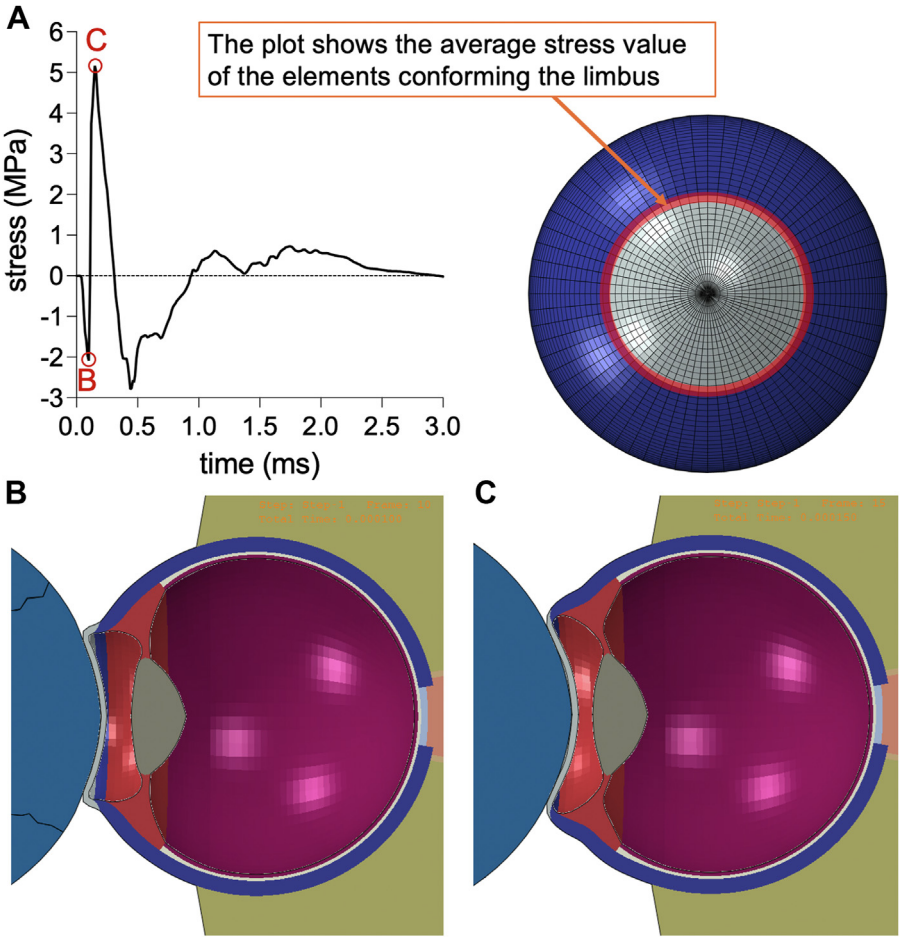


**Figure 3.** Time course of principal stress sustained by the limbus. **A,** Elements at the junction of cornea and sclera, corresponding to the limbus, were measured for stress upon shuttlecock impact. The stress plot in panel A demonstrates an immediate compressive stress of around 2 MPa (point B for panel B visual), followed by a maximal tensile stress of around 5 MPa (point C for panel C visual). **B,** Simulation of model eye at point B shows corneal buckling from impact that transfers compressive forces to the limbus. **C,** Simulation of model eye at point C shows continued corneal buckling that stresses the limbus.

the zonular fibers of 7 MPa with this maximal displacement, as well as a maximal stretch of 52% of the original length of the zonular fiber, typically around 1 mm.[36,37] After the initial lens displacement and zonular fiber stretching, the lens rebounds for a second posterior displacement event of nearly a similar degree, but with less tensile stress and strain on the zonular fibers due to anterior scleral deformations.

Compression of the aqueous humor by the shuttlecock impact induces a very brief (<1 ms) peak IOP in the anterior chamber of 5.7 MPa ($42.7 \times 10^3$ mmHg) in front of the lens that distributes radially and compresses the ciliary body for a stress of nearly 0.5 MPa (Fig 5). The resulting posterior lens displacement also transfers the peak pressure to the vitreous humor. The stretching of the zonules/lens also contributes to the ciliary deformations. As the IOP in both the aqueous and vitreous humors distribute radially, the ciliary body is stretched with a peak tensile stress of nearly 2 MPa (Fig 5). The lens rebounds, displacing anteriorly and inducing an increase in IOP in the anterior chamber again. Meanwhile, the vitreal pressure continues its movement radially toward the ora serrata. Tensile stress within the ciliary body is alleviated as the direction of pressure waves from the aqueous and vitreous humor oppose each other. With scleral contraction and consequent deformations, the ciliary tensile stresses oscillate but also dissipate. Intraocular pressure eventually distributes posteriorly toward the optic nerve head. The corresponding simulations of ciliary body stress are shown in supplementary media S4 (available at www.ophthalmologyscience.org).

Stresses at the junction between the ciliary body and retina, namely the ora serrata, were also examined (Fig 6). Upon shuttlecock impact, resultant ocular deformations/distortions, such as corneal buckling, as well as radial distribution of pressure from aqueous humor, contribute to peak radial tensile stresses at the ora serrata of 0.62 MPa. Simultaneously, the retinal aspect of the ora serrata sustains a maximal compressive stress of 0.57 MPa due to limbal ocular deformations and IOP accumulation in the vitreous humor (Fig 6). Both also contribute to the slow decline in this compressive retinal stress. Pressure that had

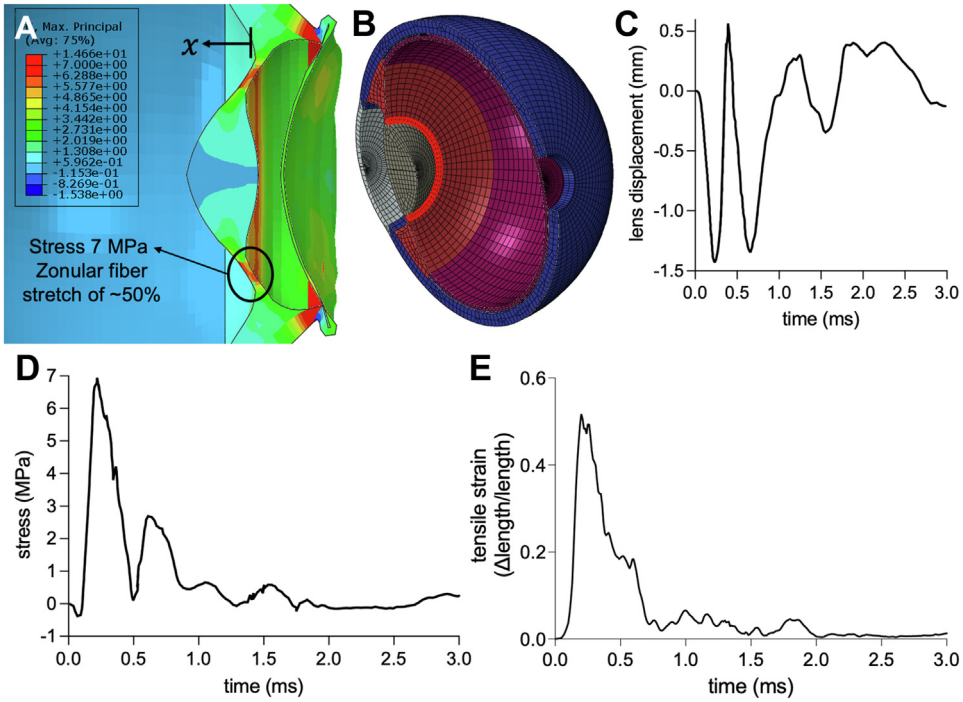


**Figure 4.** Zonular fiber stress with lens displacement. **A,** Peak zonular fiber stress of 7 MPa at 0.20 ms after shuttlecock impact. **B,** Elements between the lens and ciliary body, corresponding to zonules, were measured for stress upon shuttlecock impact. **C,** Lens displacement plot with maximal displacement of 0.5 mm with subsequent rebounding displacement events. **D,** Zonular fiber stress plot with initial peak amplitude of 7 MPa with subsequent lower intensity waves. **E,** Zonular fibers experience a maximal stretch of 52% of its original length around 1 mm.

been transferred to the vitreous humor eventually distributes radially, reaching the ora serrata, contributing to a peak compressive stress at the ora serrata of 0.57 MPa. As IOP from the vitreous humor progresses posteriorly and with greater scleral deformation, tensile stress at the ora serrata reemerges at a lower intensity of around 0.36 MPa but is slower to dissipate.

As pressure in the vitreous humor distributes posteriorly and with scleral contraction, the retina endures compressive stresses. The retina at the peripheral equator experiences a compressive stress of up to 0.23 MPa, with pressure from the vitreous humor of up to 0.27 MPa (Fig 7A-B). At the posterior pole, the retina experiences a compressive stress of up to 0.54 MPa, with pressure from the vitreous humor of up to 0.40 MPa (Fig 7C-D). Pressure from the vitreous humor contributes most significantly to the compressive stress sustained by the retina, demonstrated by the reciprocity in the behavior of the curves of pressure and stress with similar amplitudes (Fig 7). The corresponding simulations of retinal stress at the peripheral equator and posterior pole are shown in supplementary media S5 and S6 (available at www.ophthalmologyscience.org).

Furthermore, given the stiffness of the sclera, the transmission of force to the optic nerve head was faster through the sclera than the vitreous. The transmission of compressive force through the sclera posteriorly eventually caused a compressive stress of 6 MPa at the periphery of the lamina cribrosa sclerae (Fig 8A-B). Meanwhile, the impact transmitted through the posterior chamber led to the maximal posterior displacement of the optic nerve head of 2.6 mm, around 10% the axial length of a human eye (Fig 8C-D).

## Discussion

The complications after badminton-related ocular trauma reported by various studies with ≥10 subjects are: hyphema (12.7%−95.7%), traumatic angle recession (33.3%−73.9%), traumatic mydriasis (16.7%−54.1%), delayed secondary glaucoma (37.3%−42.4%), lens subluxation (17.4%−31.4%), traumatic uveitis (25.0%), corneal abrasion (13.0%−22.5%), commotio retinae (21.7%), iridodialysis (17.6%), vitreous hemorrhage (5.9%−17.4%), traumatic cataracts (4.9%−9.4%), retinal detachment or dialysis (2.4%−15.7%), cyclodialysis (5.9%−7.8%), and retinal hole (2.0%).[3,4,10] Optic nerve avulsion or injury has also been reported.[15] Most cases of shuttlecock eye trauma are closed-globe injuries.[2,3,14] Corneal, limbal, or scleral tears, especially from blunt force trauma, are rare given their composition, possessing majority type I collagen, which has an estimated maximal tensile strength of 100 to 580 MPa.[38,39]

In our FEA simulations, forces were quickly transmitted through structures with high stiffness, such as the cornea and sclera. The aqueous and vitreous humors, which have low compressibility, also played a role in transmitting forces throughout the globe. Ocular structural deformations or distortions led to distribution of IOP differentially throughout the eye, which ultimately contributed to tensile

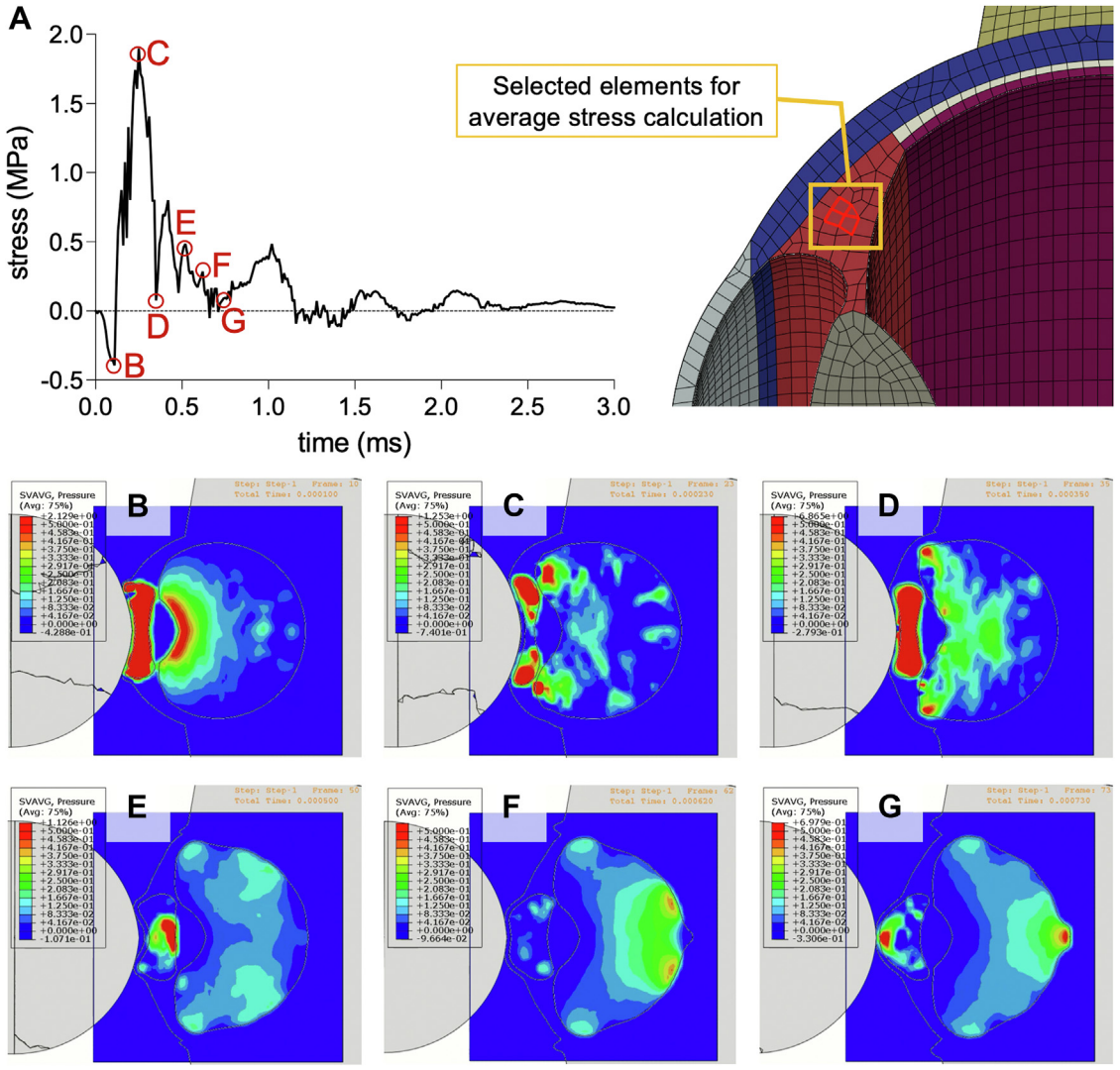


**Figure 5.** Ciliary body stress. **A,** Internal elements of the ciliary body were measured for stress upon shuttlecock impact. The ciliary body undergoes an initial compressive stress up to nearly 0.39 MPa (point B for panel B visual), followed by building tensile stress of up to nearly 2 MPa (point C for panel C visual). Gradually, stress dissipates as it also oscillates in tensile amplitude or strength. Panels **B** to **G** display the IOP distribution at different time points indicated on the ciliary body stress plot. **B,** Initial impact induces a peak IOP of 5.66 MPa in the anterior chamber that distributes through the aqueous humor, inducing compressive stress on the ciliary body. The resulting lens displacement transfer compressive forces to the vitreous humor. **C,** The IOP distributed radially in the aqueous and vitreous humors induce tensile stress upon the ciliary body. **D,** The lens rebounds anteriorly causing a rise in IOP in the anterior chamber. Stress is temporarily alleviated in the ciliary body, as the direction of pressures from the aqueous and vitreous humors negate each other. **E,** Scleral buckling is more apparent and tensile stresses on the ciliary body increase again but to a lesser extent. IOP is more concentrated in front of the lens at around 1.13 MPa, less than the initial 5.66 MPa sustained upon shuttlecock impact. **F,** IOP distributes more posteriorly, and ciliary stress has now greatly dissipated. **G,** IOP continues to advance posteriorly down to the optic nerve head as ciliary stress also continues to decrease. IOP = intraocular pressure.

or compressive stresses on various vulnerable ocular structures, such as the zonular fibers, ciliary body, ora serrata, retina, and optic nerve.

Compressive stresses at the limbus are clinically significant to the cornea due to potential damage to corneal stem cells at the limbus, leading to a longer recovery for corneal abrasions, which were present in around one-fifth of patients presenting to the clinic after badminton-related ocular injury.[3,4,10] Furthermore, structures beneath the limbus, such as the trabecular meshwork and ciliary body, are also vulnerable to injury. Our simulations demonstrate the transfer of stresses to the ciliary body but not the trabecular meshwork, which will be included in future models when its material properties are better understood experimentally.

Zonular fibers, which are connected to the ciliary body, stabilize the lens and contribute to accommodation. In our simulations, the compressive pressure from the aqueous humor after shuttlecock impact led to a posterior displacement of the lens and zonules. Concurrently, trauma compresses the eye in the anterior-posterior direction, causing expansion equatorially, thereby further stretching the

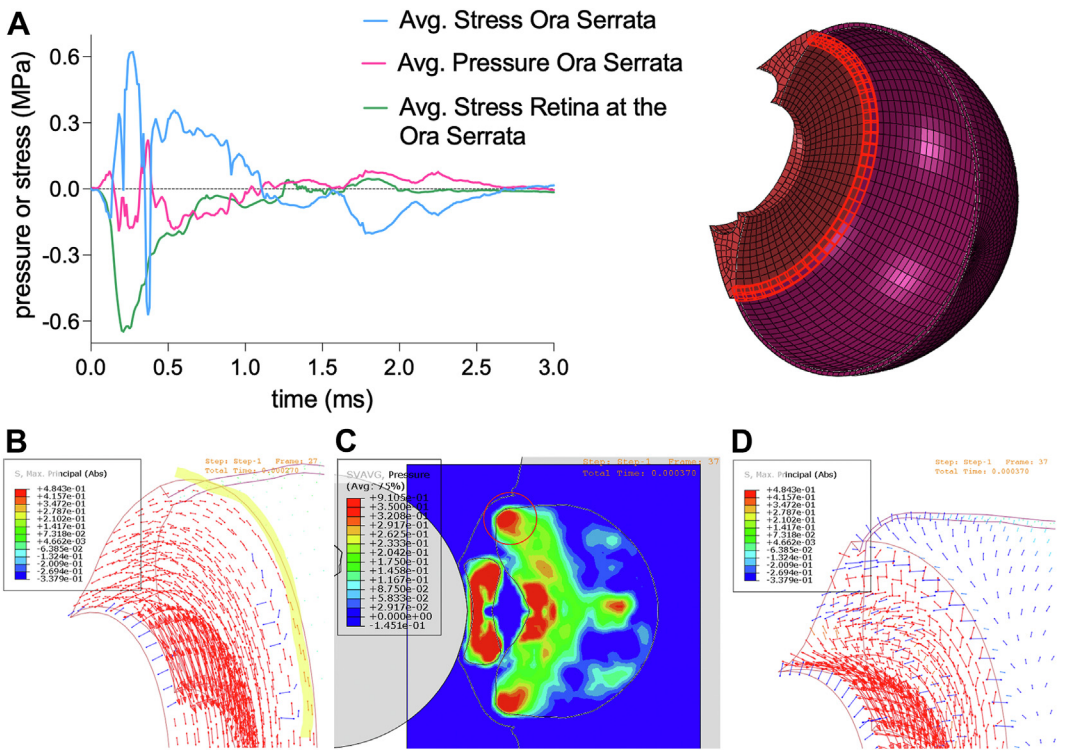


**Figure 6.** Ora serrata pressure and stress. **A,** Elements at the junction of the ciliary body and retina, corresponding to the ora serrata, were measured for stress upon shuttlecock impact. The initial compressive stress on the ora serrata of up to 0.13 MPa corresponds to a contribution of 0.08 MPa in IOP transmitted from the aqueous humor. **B,** Subsequent ocular deformations/distortions along with IOP pressures of 0.18 MPa contribute to radial/circumferential tensile stresses of up to 0.62 MPa. The red arrows represent tensile stresses, while the blue arrows represent compressive stresses. While the ora serrata experience tensile stress, the retinal portion experiences a peak compressive stress around 0.65 MPa from ocular deformations at the limbus and accumulation of IOP from the vitreous humor, which both contribute to the slow decline in this compressive retinal stress. **C** to **D,** Eventually, IOP from vitreous humor induces compressive stresses at the ora serrata, with a peak stress of 0.57 MPa; meanwhile, internal elements of the ciliary body still experience tensile stresses that have not yet alleviated. As the IOP from the vitreous humor distributes posteriorly, the tensile stresses on the ora serrata return. IOP = intraocular pressure.

zonules. The ocular deformations and lens displacement led to zonular fiber tensile stress, peaking at 7 MPa, while stretching up to 52% of its original length of around 1 mm. Zonular fibers are composed of fibrillin, providing elasticity, allowing stretching of up to around 4 mm, depending on age.[40,41] However, the maximal elastic strain upon which irreversible supra-structural zonular defects arise is at around >80% of its original length.[42,43] Notably, physiological strain from lens accommodation is only at around 3% of its resting length.[42] Given the speed of our shuttlecock being lower than the average speed mid-flight in a professional setting, the risk of lens subluxation can be substantial at higher levels of competition. It is also not uncommon for players to converge with a badminton smash. Furthermore, there could be an unrecognized subclinical defect in the zonules that may result in an inability to withstand even a 1-mm distention.

Stresses at the iridocorneal angle are particularly significant to many of the complications listed, including angle recession, hyphema, mydriasis, and cyclodialysis.[3,4,10] These complications also contribute to angle recession glaucoma, which often occurs with blunt force trauma.[44] Angle recession glaucoma may take years and decades to develop and is thought to be due to microtrauma sustained by the trabecular meshwork and distal intrascleral outflow channels causing a rise in outflow resistance over time. The initial compressive force to the anterior chamber from shuttlecock impact led to a brief (<1 ms) instance of pressure in front of the lens of 5.66 MPa ($42.5 \times 10^3$ mmHg) that radially distributed toward the trabecular meshwork of the iridocorneal angle for a brief instance of pressure of 1.25 MPa ($9.4 \times 10^3$ mmHg) (Fig 5). Therefore, at these pressures, though exceedingly brief, the high likelihood of traumatic angle recession is plausible.[45] Considering the high likelihood of damage to the trabecular meshwork, gonioscopy is highly recommended during patient serial evaluations.[45]

Pressure and consequent stresses distributed to the ciliary body can lead to hyphema and traumatic mydriasis. Hyphema can also contribute to secondary glaucoma due to trabecular meshwork obstruction with cellular or microthrombi debris. The elastic stress or strain limits of the ciliary body has not yet been clearly experimentally determined; however, given its large composition of smooth muscle tissue, the elastic stress limits of other tissue with significant composition of smooth muscle, such as gastrointestinal, vascular, or respiratory tissue, can be referenced, with a limit ranging from 0.4 to 2.3 MPa.[46–48] Our model shows a peak ciliary tensile stress of 2 MPa, which is around the elastic stress limit of smooth muscle tissue (Fig 5).

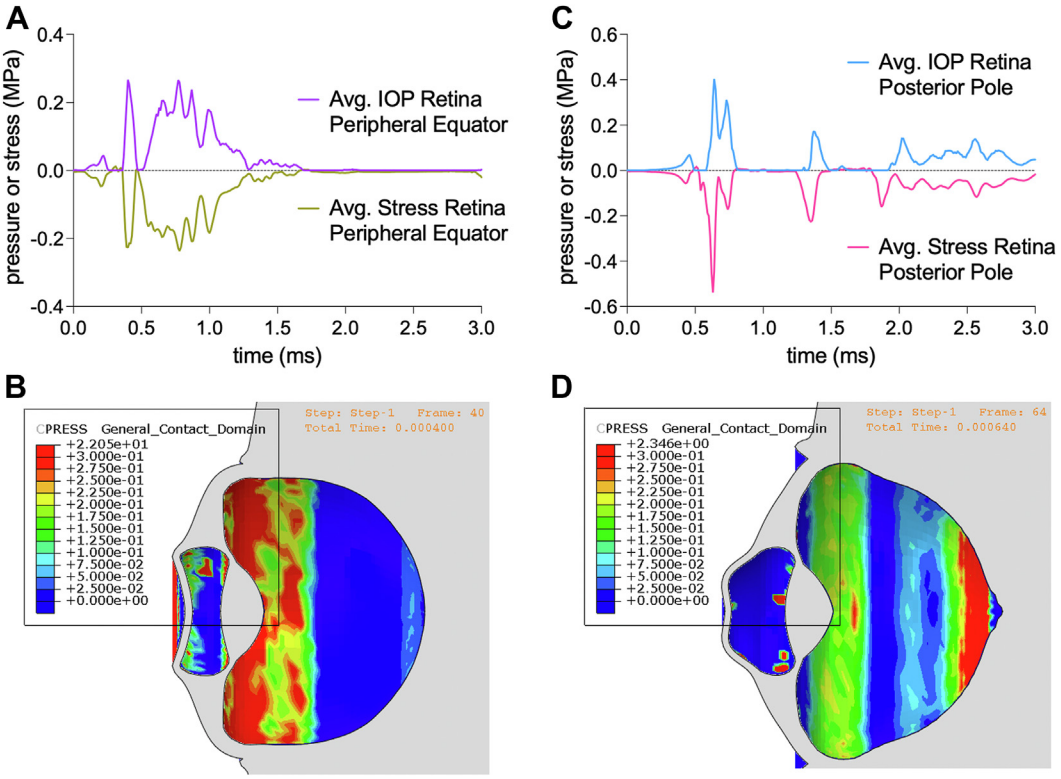


**Figure 7.** Pressure and stress on retina at peripheral equator and posterior pole. **A,** Stress plot of the retina at the peripheral equator behaves reciprocally to the IOP plot, with a peak compressive stress of 0.23 MPa and IOP of 0.27 MPa. **B,** Heatmap of IOP from vitreous humor sustained by the retina with pressures reaching the peripheral equator. **C,** Stress plot of the retina at the posterior pole behaves reciprocally to the IOP plot, with a peak compressive stress of 0.54 MPa and IOP of 0.40 MPa. **D,** Heatmap of IOP from vitreous humor sustained by the retina with pressures reaching the posterior pole. IOP = intraocular pressure.

Therefore, at higher shuttlecock velocity, the ciliary body can be subject to significant damage from tensile stress. Before the tensile stress due to IOP and ocular distortions, the ciliary body endures an initial compressive stress of 0.39 MPa (Fig 5). This compression can potentially contribute to cell death of various tissue types within the ciliary body, such as smooth muscle, neural, and epithelial tissue.[49–52] Our simulations, demonstrating this initial compression followed by the much larger stretching of tissue, elucidate the mechanism of injury to the ciliary body.

At the junction of the ciliary body and retina, the ora serrata also experiences an initial compression of 0.13 MPa followed by a tensile stress of up to 0.62 MPa (Fig 6). The retina has very soft material properties, given that neural tissue has a Young's modulus of around 100 Pa to 10 kPa[53,54] and a maximal stress limit of around 100 to 500 Pa.[55,56] Therefore, the ora serrata, being composed of both ciliary and retinal components, can be at significant risk of tearing or damage. The retina at the ora serrata mostly experiences compressive stress (max 0.65 MPa) that is greater than that endured by the retina at the peripheral equator (max 0.23 MPa) or the posterior pole (max 0.54 MPa) (Fig 7). While the retina at the ora serrata is compressed, the ciliary body is undergoing tensile stress. The differential of compression at the retina and tension at the ciliary body can serve as the mechanistic basis of retinal dialysis and detachment at the ora serrata after blunt ocular trauma.[57] Given the sensitivity of nervous tissue to compressive forces, the pressure on the retina can also contribute to neural or vascular cell death, contributing to commotio retinae, and increasing retinal tissue susceptibility to future dialysis or detachment.[58,59]

As the compressive forces transmit through the vitreous humor posteriorly, the optic nerve head is compressed up to 7.99 MPa, with a maximum posterior displacement of 2.6 mm (Fig 8). Furthermore, before the compression from the vitreous humor, compressive forces are transmitted even faster through the sclera leading to scleral wrinkling and constriction of the optic nerve head and lamina cribrosa, with a stress of up to nearly 6 MPa. Notably, the lamina cribrosa is a major site of axonal injury, causing retinal ganglion cell death in glaucoma.[60,61] A case of optic nerve avulsion and injury from shuttlecock impact has previously been reported.[15] Compressive forces leading to axonal injury and retinal cell death can help elucidate the dramatic reduction in visual acuity, even after partial recovery.[3,5,7]

Our FEA model demonstrated the injury mechanism in different ocular structures upon blunt trauma from shuttlecock impact. However, our study has several limitations of consideration. Performing traumatic injury experiments in vivo poses several ethical challenges, as well as technical

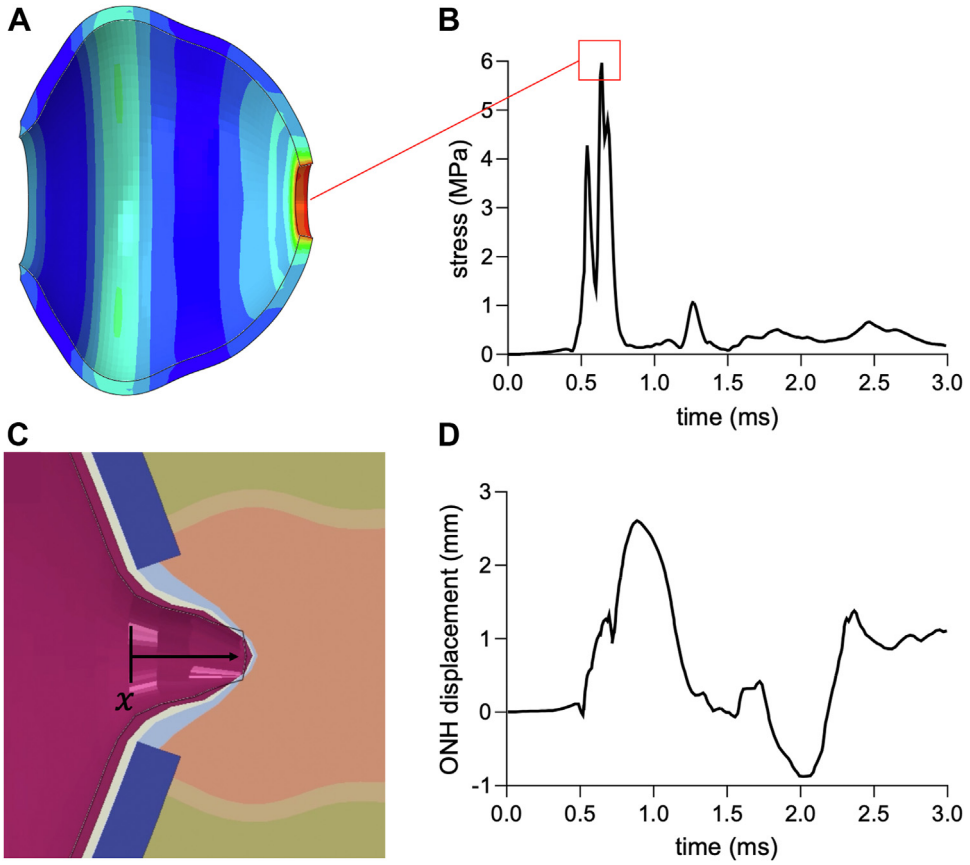


**Figure 8.** Contraction pressure at scleral optic nerve canal and displacement of ONH. **A,** Stress heatmap during peak ONH contraction pressure. **B,** Red box indicates a peak stress of 5.97 MPa at the ONH 0.64 ms after shuttlecock impact with the corresponding snapshot of stressheat map shown in panel A. **C,** Snapshot of maximal ONH displacement during simulation of ocular mechanical response to shuttlecock impact. **D,** Optic nerve head displacement plot with maximal displacement of 2.6 mm. ONH = optic nerve head.

challenges, particularly in the precise measurements of responses of ocular structures, which would be useful in validating the results from our simulations. Our model eye was based on prior designs that accounted for experimental properties from several in vitro studies and predicted properties using known values from other similar materials/tissues.[19,62] While the values for biomechanical properties of each of the relevant tissues (as presented in supplementary table 1, available at www.ophthalmologyscience.org) are based on well-established studies, there are inherent limitations in using these data. Specifically, the assumptions made regarding these properties, such as elasticity and viscosity, are derived from in vitro and ex vivo experiments. These studies provide a controlled environment, but they may not fully replicate the in vivo conditions of the human eye, where factors such as blood flow, physiologic temperature, and tissue hydration could influence the results. Our confidence in the accuracy of these values is supported by their consistency with previous finite element models cited in the literature, which have shown similar biomechanical responses.[19,22,62]

Furthermore, it is important to acknowledge the potential heterogeneity in these material properties due to variations in eye size, shape, and individual biological differences. For instance, the stiffness of the sclera or the elasticity of the lens capsule may vary significantly between individuals, affecting the overall biomechanical response to trauma. Further studies, particularly those involving direct in vivo or in situ measurements, are essential for refining these values and enhancing the predictive capability of our finite element model. The patient specific dimensions and properties of the ocular structures might affect the stress magnitude in our model, but not the anticipated stress patterns.

Our current model demonstrated peak stresses of around 5 to 6 MPa at the limbal sclera and peripapillary sclera. This peak tensile stress is close to the rupture point obtained from tensile testing of tissue.[63] However, this scleral strength is subject to variability based on individual phenotype and even more so depending on the affected scleral region, posing challenges to defining an ultimate threshold for the whole sclera. Additionally, the underlying ultrastructural mechanisms of soft tissue rupture remain unclear, limiting the ability of the FEA model to account for this response. Nonetheless, we acknowledge the viability of presenting an open globe injury after a shuttlecock insult, as previous systematic studies have highlighted its occurrence at 5% of the cases in badminton play.[2] Given the capability of our model to map stress patterns and determine stress magnitudes, future studies will involve studying a broad range of shuttlecock velocities to predict and categorize levels of associated risk.

Overall, our study demonstrates the utility of FEA to visualize and quantify the mechanical stresses and structural deformations in the ocular tissues following shuttlecock impact. Our results suggest that a direct impact from the shuttlecock could cause severe injuries and vision impairment due to its high energy transfer and small size relative to the bony orbit, facilitating extensive deformation and damage to both anterior and posterior structures. Consequent tensile and compressive stresses from shuttlecock impact nearly reach or exceed the mechanical limits of various ocular tissues, including the ciliary body, retina, and optic nerve head. These insights can inform clinical practice concerning the evaluation and treatment of ocular injuries resulting from shuttlecock impacts and possibly other blunt ocular traumas. Furthermore, our insights underscore the critical importance of preventive measures, such as protective eyewear, in averting severe ocular injuries during badminton activities. Future studies will incorporate the latest ocular tissue material properties, as we also continue to test and measure these properties with human or nonhuman primate ocular tissue. We also aim to explore the impact of shuttlecock velocity on stress magnitudes to categorize the level of associated ocular trauma risk for better awareness of the dangers at various speeds. The present study focused on the short-term direct consequences of ocular injury. Future research will aim to explore how such injuries lead to increased vulnerability to future injuries and contribute to long-term complications, such as secondary glaucoma, optic nerve damage, corneal endothelial damage, uveitis, and cataract formation.

## Footnotes and Disclosures

Originally received: June 17, 2024.
Final revision: September 1, 2024.
Accepted: September 16, 2024.
Available online 19 September 2024. Manuscript no. XOPS-D-24-00192.

[1] Department of Ophthalmology, Gavin Herbert Eye Institute, University of California, Irvine, California.

[2] Bio-Mechanics Laboratory, Department of Biomedical Engineering and Science, Florida Institute of Technology, Melbourne, Florida.

[3] Department of Ophthalmology, Tulane University School of Medicine, New Orleans, Louisiana.

[4] Department of Ophthalmology, Creighton University School of Medicine, Omaha, Nebraska.

[5] Lions Eye Institute, The University of Western Australia, Nedlands, Perth, Western Australia, Australia.

[6] Save Sight Institute, Sydney Eye Hospital, Sydney, New South Wales, Australia.

[7] National Healthcare Group Eye Institute, Tan Tock Seng Hospital, Novena, Singapore.

[8] Lee Kong Chian School of Medicine, Nanyang Technological University, Novena, Singapore.

[9] Singapore Eye Research Institute, Singapore National Eye Centre, Bukit Merah, Singapore.

[10] Department of Ophthalmology, Duke NUS Medical School, Bukit Merah, Singapore.

*Co-first authorship of the study.

Disclosure(s):

All authors have completed and submitted the ICMJE disclosures form.

The author(s) have made the following disclosure(s):

Financial Support: This research was supported in part by National Institutes of Health Training Grants 1F30EY033659-01 and T32-GM08620 to J.D.H. The authors acknowledge support from the Gavin Herbert Eye Institute at the University of California, Irvine from an unrestricted grant from Research to Prevent Blindness.

HUMAN SUBJECTS: No human subjects were included in this study. All methods were in accordance with the Declaration of Helsinki and did not involve any human or animal subjects. The UCI Institutional Review Board Committee determined the study did not qualify as human subject research and waived the requirement for informed consent.

No animal subjects were used in this study.

Author Contributions:

Conception and design: Hong, Colmenarez, Choi, Alex Suh, Andrew Suh, Lam, Hoskin, Minckler, Lin, Shahraki, Agrawal, Dong, Gu, D.W. Suh

Data collection: Hong, Colmenarez, Choi, Alex Suh, Andrew Suh, Lam, Hoskin, Minckler, Lin, Shahraki, Agrawal, Dong, Gu, D.W. Suh

Analysis and interpretation: Hong, Colmenarez, Choi, Alex Suh, Andrew Suh, Lam, Hoskin, Minckler, Lin, Shahraki, Agrawal, Dong, Gu, D.W. Suh

Obtained funding: N/A

Overall responsibility: Hong, Colmenarez, Choi, Alex Suh, Andrew Suh, Lam, Hoskin, Minckler, Lin, Shahraki, Agrawal, Dong, Gu, D.W. Suh

Abbreviations and Acronyms:
**FEA** = finite element analysis; **IOP** = intraocular pressure.

Keywords:
Sports-related injury, Ocular trauma, Glaucoma, Lens dislocation, Retinal injury.

Correspondence:
Donny W. Suh, MD, MBA, Department of Ophthalmology, Gavin Herbert Eye Institute, University of California, Irvine, 850 Health Sciences Road, Irvine, CA 92697. E-mail: donnys@hs.uci.edu.

## References

1. BWF BWFBWF Badminton World Federation. *Annual Report 2019*. Malaysia; 2019.
2. Hoskin AK, Watson S, Kamalden TA. Badminton-related eye injuries: a systematic review. *Inj Prev*. 2023;29:116–120.
3. Guo T, Shi W, Yi X, et al. Clinical evaluation and management of badminton-related eye injuries: a retrospective case series. *BMC Ophthalmol*. 2023;23:258.
4. Mohd Rasidin AH, Muhammad-Ikmal MK, Raja Omar RN, et al. Clinical audit on badminton-related ocular injuries in a tertiary hospital in Malaysia. *Cureus*. 2022;14:e30769.
5. Yu J, Chen Y, Miao J, et al. Doubles trouble-85 cases of ocular trauma in badminton: clinical features and prevention. *Br J Sports Med*. 2020;54:23–26.

6. Lee DE, Ryoo HW, Moon S, et al. Epidemiology and risk factors for sports- and recreation-related eye injury: a multicenter prospective observational study. *Int J Ophthalmol*. 2021;14:133−140.
7. Chandran S. Ocular hazards of playing badminton. *Br J Ophthalmol*. 1974;58:757−760.
8. Maldoddi R, Gella L. Eye injuries in badminton - players' perspective toward the usage of personal protective equipment. *Phys Sportsmed*. 2024;52:46−51.
9. Vinger PF. *The Mechanisms and Prevention of Sports Eye Injuries*. Massachusetts: Lexington Eye Associates; 2010.
10. Jao KK, Atik A, Jamieson MP, et al. Knocked by the shuttlecock: twelve sight-threatening blunt-eye injuries in Australian badminton players. *Clin Exp Optom*. 2017;100:365−368.
11. Nadolny M. *Shuttlecock and balls: The fastest moving objects in sport*. Toronto, Ontario, Canada: Canadian Olympic Committee; 2014.
12. Bekerman I, Gottlieb P, Vaiman M. Variations in eyeball diameters of the healthy adults. *J Ophthalmol*. 2014;2014:503645.
13. Mazarelo JFD, Winter SL, Fong DTP. A systematic review on the effectiveness of eyewear in reducing the incidence and severity of eye injuries in racket sports. *Phys Sportsmed*. 2023;52:1−10.
14. Zhang Y, Jia H, Kang X, et al. Discrepancy of eye injuries in mechanism, clinical features, and vision prognosis by different causative sports. *Front Public Health*. 2023;11:1182647.
15. Kawamata Y, Kitamura Y, Yokouchi H, Baba T. Case report: partial visual recovery from incomplete traumatic optic nerve avulsion caused by a badminton shuttle. *Am J Ophthalmol Case Rep*. 2022;27:101624.
16. Wang DN, Luong M, Hanson C. Traumatic hyphema in a 13-year-old girl: eye protection regulation in badminton is needed. *CMAJ*. 2020;192:E778−E780.
17. Luong M, Dang V, Hanson C. Traumatic hyphema in badminton players: should eye protection be mandatory? *Can J Ophthalmol*. 2017;52:e143−e146.
18. Khandelwal R, Majumdar MR, Gupta A. An unusual mechanism of ocular trauma in badminton players: two incidental cases. *BMJ Case Rep*. 2012;2012:bcr2012006363.
19. Lam MR, Yang CD, Colmenarez JA, et al. The role of intrapartum fetal head compression in neonatal retinal hemorrhage. *J AAPOS*. 2023;27:267.e1−267.e7.
20. Song HH, Thoreson WB, Dong P, et al. Exploring the vitreoretinal interface: a key instigator of unique retinal hemorrhage patterns in pediatric head trauma. *Korean J Ophthalmol*. 2022;36:253−263.
21. Lam MR, Dong P, Shokrollahi Y, et al. Finite element analysis of soccer ball-related ocular and retinal trauma and comparison with abusive head trauma. *Ophthalmol Sci*. 2022;2:100129.
22. Karimi A, Razaghi R, Rahmati SM, et al. A nonlinear dynamic finite-element analyses of the basketball-related eye injuries. *Sports Eng*. 2018;21:359−365.
23. Suh A, Lam M, Shokrollahi Y, et al. Quantifying the efficacy of protective eyewear in pediatric soccer-induced retinal injury. *J AAPOS*. 2023;27:131.e1−131.e6.
24. Suh DW, Song HH, Mozafari H, Thoreson WB. Determining the tractional forces on vitreoretinal interface using a computer simulation model in abusive head trauma. *Am J Ophthalmol*. 2021;223:396−404.
25. Tong J, Kedar S, Ghate D, Gu L. Indirect traumatic optic neuropathy induced by primary blast: a fluid-structure interaction study. *J Biomech Eng*. 2019;141:101011.
26. Zaharil NB, Ogawa K, Odaka M, Okanaga H. Aerodynamic characteristics of the badminton shuttlecock shortly. In: *The Engineering of Sport*. 14. West Lafayette: Purdue University; 2022.
27. Colmenarez JA, Zhai Y, Mendoza VO, et al. Damage-induced softening of the sclera: a pseudo-elastic modeling approach. *ASME J Med Diagn*. 2023;7:031001.
28. Zhai Y, Colmenarez JA, Mendoza VO, et al. Multiscale mechanical characterization of cornea with AFM, SEM, and uniaxial tensile test | IMECE | ASME digital collection. *ASME Int Mech Eng Congr Expo*. 2024;5. V005T06A010.
29. Tong J, Ghate D, Kedar S, Gu L. Relative contributions of intracranial pressure and intraocular pressure on lamina cribrosa behavior. *J Ophthalmol*. 2019;2019:3064949.
30. Chen K, Weiland JD. Mechanical properties of orbital fat and its encapsulating connective tissue. *J Biomech Eng*. 2011;133:064505.
31. Schoemaker I, Hoefnagel PP, Mastenbroek TJ, et al. Elasticity, viscosity, and deformation of orbital fat. *Invest Ophthalmol Vis Sci*. 2006;47:4819−4826.
32. Edwards ME, Good TA. Use of a mathematical model to estimate stress and strain during elevated pressure induced lamina cribrosa deformation. *Curr Eye Res*. 2001;23:215−225.
33. Voorhees AP, Hua Y, Brazile BL, et al. So-called lamina cribrosa defects may mitigate IOP-induced neural tissue insult. *Invest Ophthalmol Vis Sci*. 2020;61:15.
34. Franze K, Francke M, Günter K, et al. Spatial mapping of the mechanical properties of the living retina using scanning force microscopy. *Soft Matter*. 2011;7:3147−3154.
35. Wang X, Rumpel H, Lim WE, et al. Finite element analysis predicts large optic nerve head strains during horizontal eye movements. *Invest Ophthalmol Vis Sci*. 2016;57:2452−2462.
36. Pavlin CJ, Buys YM, Pathmanathan T. Imaging zonular abnormalities using ultrasound biomicroscopy. *Arch Ophthalmol*. 1998;116:854−857.
37. Remington LA, Goodwin D. *Clinical Anatomy and Physiology of the Visual System*. St. Louis, Missouri: Elsevier Butterworth-Heinemann; 2011.
38. Dutov P, Antipova O, Varma S, et al. Measurement of elastic modulus of collagen type I single fiber. *PLoS One*. 2016;11:e0145711.
39. Gouissem A, Mbarki R, Al Khatib F, Adouni M. Multiscale characterization of type I collagen fibril stress-strain behavior under tensile load: analytical vs. MD approaches. *Bioengineering (Basel)*. 2022;9:193.
40. Assia EI, Apple DJ, Morgan RC, et al. The relationship between the stretching capability of the anterior capsule and zonules. *Invest Ophthalmol Vis Sci*. 1991;32:2835−2839.
41. Bassnett S. Zinn's zonule. *Prog Retin Eye Res*. 2021;82:100902.
42. Sherratt MJ, Baldock C, Haston JL, et al. Fibrillin microfibrils are stiff reinforcing fibres in compliant tissues. *J Mol Biol*. 2003;332:183−193.
43. Baldock C, Koster AJ, Ziese U, et al. The supramolecular organization of fibrillin-rich microfibrils. *J Cell Biol*. 2001;152:1045−1056.
44. Ng JK, Lau O. Traumatic Glaucoma. In: *StatPearls*. Treasure Island, FL: StatPearls Publishing; 2023.
45. Herschler J. Trabecular damage due to blunt anterior segment injury and its relationship to traumatic glaucoma. *Trans Sect Ophthalmol Am Acad Ophthalmol Otolaryngol*. 1977;83:239−248.
46. Trabelsi O, del Palomar AP, Lopez-Villalobos JL, et al. Experimental characterization and constitutive modeling of the mechanical behavior of the human trachea. *Med Eng Phys*. 2010;32:76−82.

47. Ohashi T, Sugita S, Matsumoto T, et al. Rupture properties of. blood vessel walls measured by pressure-imposed test. *Jsme Inter J Ser C Mech Sys Mac Elem Manuf Q*. 2003;46: 1290−1296.
48. Massalou D, Masson C, Afquir S, et al. Mechanical effects of load speed on the human colon. *J Biomech*. 2019;91:102−108.
49. Hehrlein C, Weinschenk I, Metz J. Long period of balloon inflation and the implantation of stents potentiate smooth muscle cell death. Possible role of chronic vascular injury in restenosis. *Int J Cardiovasc Intervent*. 1999;2:21−26.
50. Lotz JC, Chin JR. Intervertebral disc cell death is dependent on the magnitude and duration of spinal loading. *Spine*. 2000;25: 1477−1483.
51. Takao S, Taya M, Chiew C. Mechanical stress-induced cell death in breast cancer cells. *Biol Open*. 2019;8: bio043133.
52. Bar-Kochba E, Scimone MT, Estrada JB, Franck C. Strain and rate-dependent neuronal injury in a 3D in vitro compression model of traumatic brain injury. *Sci Rep*. 2016;6:30550.
53. Green MA, Bilston LE, Sinkus R. In vivo brain viscoelastic properties measured by magnetic resonance elastography. *NMR Biomed*. 2008;21:755−764.
54. Lacour SP, Courtine G, Guck J. Materials and technologies for soft implantable neuroprostheses. *Nat Rev Mater*. 2016;1:1−14.
55. Budday S, Sommer G, Birkl C, et al. Mechanical characterization of human brain tissue. *Acta Biomater*. 2017;48: 319−340.
56. Miller K, Chinzei K. Mechanical properties of brain tissue in tension. *J Biomech*. 2002;35:483−490.
57. Rohowetz LJ, Jabbehdari S, Smiddy WE, et al. Retinal detachment associated with retinal dialysis: clinical features and outcomes of surgery in a 10-year study. *Ophthalmol Retina*. 2023;7:857−861.
58. LaPlaca MC, Simon CM, Prado GR, Cullen DK. CNS injury biomechanics and experimental models. *Prog Brain Res*. 2007;161:13−26.
59. Quan X, Guo K, Wang Y, et al. Mechanical compression insults induce nanoscale changes of membrane-skeleton arrangement which could cause apoptosis and necrosis in dorsal root ganglion neurons. *Biosci Biotechnol Biochem*. 2014;78:1631−1639.
60. Minckler DS, Bunt AH, Johanson GW. Orthograde and retrograde axoplasmic transport during acute ocular hypertension in the monkey. *Invest Ophthalmol Vis Sci*. 1977;16: 426−441.
61. Minckler D, Stamper R, Han Y, et al. Axonal transport in coats' disease and congenital oculodentodigital syndrome. *J Neurol Transl Neurosci*. 2023;8:1−6.
62. Razaghi R, Biglari H, Karimi A. Finite element modeling of the eyeglass-related traumatic ocular injuries due to high explosive detonation. *Eng Fail Anal*. 2020;117:104835.
63. Colmenarez JA, Zhai Y, Mendoza VO, et al. Damage-Induced Softening of the Sclera: A Psuedo-Elastic Modeling Approach. *J Eng Sci Med Diagnostics Ther*. 2024;7.